Organic & Biomolecular Chemistry

PAPER

View Article Online
View Journal | View Issue

Cite this: *Org. Biomol. Chem.*, 2014, **12**, 5936

New multi-target-directed small molecules against Alzheimer's disease: a combination of resveratrol and clioquinol†

Fei Mao,[a] Jun Yan,[a] Jianheng Li,[a] Xian Jia,[b] Hui Miao,[a] Yang Sun,[a] Ling Huang*[a] and Xingshu Li*[a]

Received 14th May 2014,
Accepted 13th June 2014

DOI: 10.1039/c4ob00998c

www.rsc.org/obc

Alzheimer's disease (AD) is currently one of the most difficult and challenging diseases to treat. Based on the 'multi-target-directed ligands' (MTDLs) strategy, we designed and synthesised a series of new compounds against AD by combining the pharmacophores of resveratrol and clioquinol. The results of biological activity tests showed that the hybrids exhibited excellent MTDL properties: a significant ability to inhibit self-induced β-amyloid (Aβ) aggregation and copper(II)-induced Aβ aggregation, potential antioxidant behaviour (ORAC-FL value of 0.9–3.2 Trolox equivalents) and biometal chelation. Among these compounds, (*E*)-5-(4-hydroxystyryl)quinoline-8-ol (**10c**) showed the most potent ability to inhibit self-induced Aβ aggregation (IC_{50} = 8.50 μM) and copper(II)-induced Aβ aggregation and to disassemble the well-structured Aβ fibrils generated by self- and copper(II)-induced Aβ aggregation. Note that **10c** could also control Cu(I/II)-triggered hydroxyl radical ($OH^{\bullet}$) production by halting copper redox cycling *via* metal complexation, as confirmed by a Cu–ascorbate redox system assay. Importantly, **10c** did not show acute toxicity in mice at doses of up to 2000 mg kg^{-1} and was able to cross the blood–brain barrier (BBB), according to a parallel artificial membrane permeation assay. These results indicate that compound **10c** is a promising multifunctional compound for the development of novel drugs for AD.

Introduction

Alzheimer's disease (AD), which was first described by Alois Alzheimer in 1906,[1–3] is currently one of the most difficult and baffling diseases to treat. The characteristic symptom of AD is the progressive loss of memory and other cognitive functions that invariably cause a decline in an individual's ability to function in society. AD occurs more frequently in elderly people, and it is believed that 35.6 million people suffered from AD in 2010. Note that the number of patients is predicted to nearly double every 20 years to 65.7 million in 2030 and 115.4 million in 2050.[4]

In recent decades, much evidence has suggested that AD is a multifaceted illness. In addition to the low levels of acetylcholine (on the basis of which acetylcholinesterase inhibitors, such as tacrine, donepezil, rivastigmine and galantamine, have been developed as the main therapeutic options for the treatment of AD), the following are also important in the aetiology of AD: β-amyloid (Aβ) deposits, τ-protein aggregation, oxidative stress and the dyshomeostasis of biometals.[5–7] Therefore, a more appropriate approach to addressing the multifaceted nature of AD may be the development of multi-target-directed ligands (MTDLs).[8,9]

The extracellular senile plaques and intracellular neurofibrillary tangles formed by hyperphosphorylated τ-protein are the key pathological markers of AD. Because β-amyloid peptide (Aβ) is the main component of senile plaques, the "amyloid hypothesis" proposes that the production and accumulation of the oligomeric aggregates of Aβ in the brain are the central event in the pathogenesis of AD and these aggregates initiate the pathogenic cascade that ultimately leads to neuronal loss and dementia.[10] Therefore, some anti-Aβ aggregation compounds have been identified for the treatment of AD.[11–14]

Recent studies have indicated that the dysregulation of brain metal ion homeostasis, especially that of copper and zinc, may play a very important role in the pathogenesis of AD. Zinc(II) and copper(II) were found to be markedly enriched in plaque amyloid, and were confirmed to coordinate to histidine residues in senile plaque (SP) cores by Raman microscopy.[15] While copper and zinc accumulate in the extracellular plaque,

[a]*School of Pharmaceutical Sciences, Sun Yat-sen University, Guangzhou 510006, China. E-mail: huangl72@mail.sysu.edu.cn, lixsh@mail.sysu.edu.cn; Fax: +86-20-3994-3051+86-20-3994-3050; Tel: +86-20-3994-3051+86-20-3994-3050*
[b]*School of Pharmaceutical Engineering, Shenyang Pharmaceutical University, Shenyang 110016, China*

†Electronic supplementary information (ESI) available. See DOI: 10.1039/c4ob00998c

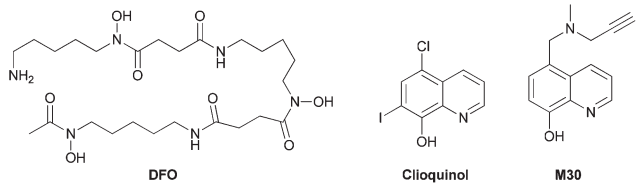

Fig. 1 Chemical structure of metal-chelating agents.

the intracellular copper stores are deficient in AD patients and can promote the generation of Aβ, leading to a vicious cycle of plaque formation and metal ion accumulation.[16] Therefore, the modulation of these biometals in the brain has been proposed to be a potential therapeutic strategy for the treatment of AD.[17] Considering this proposal, biometal chelators such as desferrioxamine (DFO), EDTA, clioquinol, and 5-[*N*-methyl-*N*-propargylaminomethyl]-8-hydroxyquinoline (M30) (Fig. 1) have been studied.[18]

Intracellular oxidative stress is one of the earliest events in the pathogenesis of AD.[19] Neuronal tissue is very sensitive to oxidative stress, and an imbalance in pro-oxidant *vs.* antioxidant homeostasis in the CNS results in the production of several potentially toxic reactive oxygen species (ROS), which play a prominent role in several neurodegenerative diseases, similar to microorganisms in infectious diseases.[20] Antioxidant protection is necessary during aging, especially in AD patients, because endogenous antioxidant protection rapidly declines. A recent statistical study involving developed countries indicated that a higher consumption of dietary antioxidants, such as flavonoids, is associated with the lower rates of dementia.[21] Thus, drugs that specifically scavenge oxygen radicals could be useful for either the prevention or the treatment of AD.[22,23]

The antioxidant properties of resveratrol have been thoroughly demonstrated and are associated with a wide range of biological effects. Fortunately, this compound has also been reported to cause no adverse effects.[24] In addition, recent papers emphasise the Aβ anti-aggregative and cytoprotective properties of resveratrol in human neuroblastoma cells.[25,26] Despite these positive effects, the poor bioavailability of dietary supplements of resveratrol severely limits its use.[27]

Evidence suggests that the most successful treatment strategy will likely incorporate a sequential and multifactorial approach.[9] Recently, multifunctional compounds targeting metal-induced Aβ aggregation have been extensively studied for AD treatments[28–30] such as a hybrid of 6-chlorotacrine and a metal-Aβ modulator reported by Lim and coworkers that inhibits acetylcholinesterase and metal-free/metal-induced Aβ aggregation.[31] In addition, Green *et al.* reported a pyclen derivative with enhanced antioxidant properties.[32] Our approach to the identification of novel multi-target-directed drug candidates for the treatment of AD is to develop multifunctional compounds that can simultaneously inhibit Aβ aggregation, modulate the dyshomeostasis of biometals, and manage oxidative stress. In this paper, we combined resveratrol with the pharmacophore moiety of the well-known metal chelator clioquinol (CQ) to obtain a series of 8-hydroxyquinoline-resveratrol derivatives that are expected to acts as biometal chelators, antioxidants, and inhibitors of Aβ aggregation (Fig. 2).

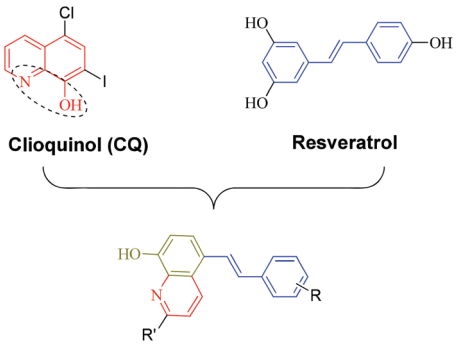

Fig. 2 Design strategy for multifunctional chelators.

Results and discussion

Chemistry

The target compounds **10a–10e**, **10g**, **13a–e** and **13h–13i** were synthesised according to the synthetic approaches depicted in Schemes 1 and 2. First, aldehyde **2** was protected with a methoxymethyl (MOM) group through the reaction of 4-hydroxybenzaldehyde with chloro(methoxy)methane in the presence of diisopropylethylamine. The reaction of methyl 3,5-dihydroxybenzoate (**3**) and chloro(methoxy)methane provided an intermediate **4**, which was reduced with $LiAlH_4$ and then oxidised using PCC to give the MOM-protected aldehyde **5**. Alternatively, 8-hydroxyquinoline or its analogue 2-methyl-8-hydroxyquinoline reacted with formaldehyde and concentrated

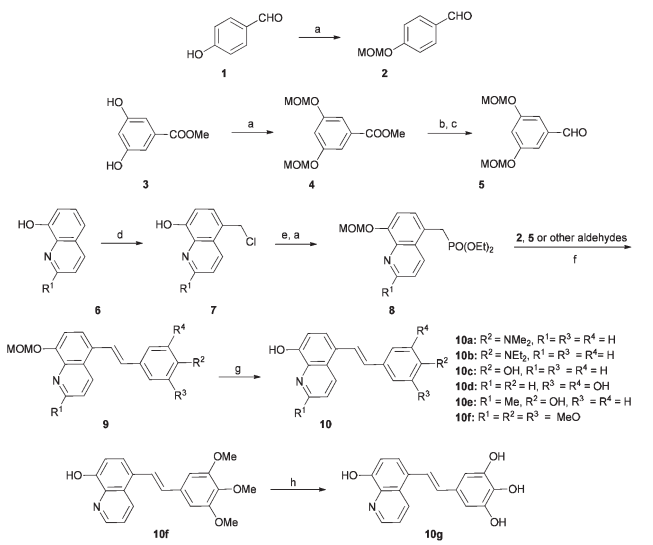

Scheme 1 Reagents and conditions: (a) MOMCl, $(i\text{-}Pr)_2NEt$, CH_2Cl_2, 0 °C to r.t.; (b) $LiAlH_4$, THF, 0 °C to r.t.; (c) PCC, CH_2Cl_2; (d) HCl (37% in water), HCHO (37% in water), 0 °C to r.t.; (e) $P(OEt)_3$, reflux; (f) CH_3ONa, DMF, 0 °C to 80 °C; (g) 6 M HCl, CH_3OH, reflux; (h) BBr_3, CH_2Cl_2, −78 °C to r.t.

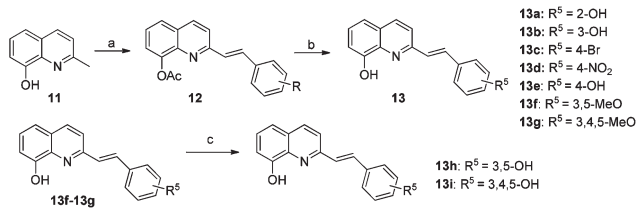

Scheme 2 Reagents and conditions: (a) aldehydes, Ac_2O, Ar, 130 °C; (b) HCl (37% water), DMF, 100 °C; (c) BBr_3, CH_2Cl_2, −78 °C to r.t.

hydrochloric acid and provided **7**. Compound **7** was reacted with triethyl phosphite and then chloro(methoxy)methane to give the Wittig reagent **8**, which was then reacted with **2**, **5**, amino-substituted aldehydes or 3,4,5-trimethoxybenzaldehyde to provide **9**. Finally, compounds **10a–10f** were obtained by deprotecting **9** in the presence of hydrochloric acid, and compound **10g** was obtained by the demethylation of compound **10f** in the presence of boron tribromide at −78 °C (Scheme 1).

2-Methyl-8-hydroxyquinoline was treated with nitro-, bromine-, hydroxyl- or methoxy-substituted benzaldehydes in the presence of acetic anhydride, followed by deacetylation with hydrochloric acid to provide **13a–13g**. Compounds **13h** and **13i** were obtained by the demethylation of the corresponding dimethoxy compounds **13f** and **13g** in the presence of boron tribromide at −78 °C (Scheme 2).

Inhibition of self-mediated $A\beta_{1-42}$ aggregation

To evaluate the inhibitory activities of 8-hydroxyquinoline-resveratrol derivatives against self-mediated $A\beta_{1-42}$ aggregation, a thioflavin-T (ThT) fluorescence binding assay[33] was performed, and resveratrol, a known amyloid aggregation inhibitor, was used as a reference compound. The results in Table 1 show that most of the synthesised compounds exhibited moderate to good potencies compared to resveratrol. Among them, compounds **10a–10d** and **10g**, which feature amino groups or hydroxyl groups on the B-ring and do not have a substituent (R^2 = H) on the A-ring, exhibited similar or better inhibition of Aβ aggregation (52.85%–71.69%, 20 μM) than resveratrol (64.57%, 20 μM). Alkyl groups on the A-ring appear to be unfavourable for inhibition, as illustrated by compound **10e**, which has a methyl group at the R^1-position of the A-ring and a hydroxyl at the R^2-position, and showed only 49.38% inhibition of Aβ aggregation at 20 μM. Compound series **13**, derived from 2-methyl-8-hydroxyquinoline and aromatic aldehydes, exhibited a similar inhibition compared with compound series **10**. For instance, compounds **13e** and **13h–13i**, which have hydroxyl groups on the C-ring, showed a 67.46–75.31% inhibition at 20 μM. The results also showed that the inhibitory activity of *para*-hydroxyl substitutions at the C-ring was better than hydroxyl substitutions at the *ortho*- or *meta*-positions (the ability of compounds **13a**, **13b** and **13e** to inhibit Aβ aggregation was 49.21%, 45.87% and 67.46%,

Table 1 Inhibition of $A\beta_{1-42}$ aggregation and oxygen radical absorbance capacity (ORAC, Trolox Equivalents) by resveratrol, CQ and 8-hydroxyquinoline-resveratrol derivatives **10a–10e**, **10g**, **13a–e** and **13h–13i**

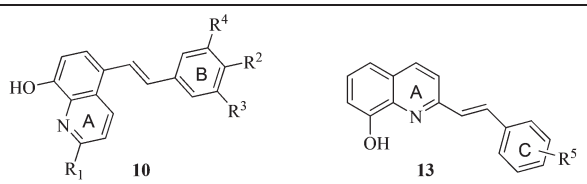

Compounds	Substituents	Inhibition of $A\beta_{1-42}$ aggregation[a] (%)	IC_{50}[b] (μM)	ORAC[d]
10a	$R^2 = NMe_2$, $R^1 = R^3 = R^4 = H$	52.85 ± 4.21	18.14 ± 1.51	1.92 ± 0.16
10b	$R^2 = NEt_2$, $R^1 = R^3 = R^4 = H$	57.76 ± 3.43	12.19 ± 1.02	2.81 ± 0.22
10c	$R^2 = OH$, $R^1 = R^3 = R^4 = H$	71.69 ± 2.42	8.50 ± 0.35	2.18 ± 0.12
10d	$R^1 = R^2 = H$, $R^3 = R^4 = OH$	69.52 ± 3.27	9.26 ± 0.56	2.52 ± 0.10
10e	$R^1 = Me$, $R^2 = OH$, $R^3 = R^4 = H$	49.38 ± 2.72	n.t.[c]	1.87 ± 0.13
10g	$R^1 = R^2 = R^3 = OH$	69.53 ± 3.70	8.98 ± 0.82	n.t.[c]
13a	R^5 = 2-OH	49.21 ± 3.36	n.t.[c]	3.16 ± 0.28
13b	R^5 = 3-OH	45.87 ± 4.22	n.t.[c]	3.22 ± 0.22
13c	R^5 = 4-Br	18.18 ± 1.35	n.t.[c]	0.93 ± 0.05
13d	$R^5 = 4\text{-}NO_2$	22.33 ± 2.14	n.t.[c]	0.91 ± 0.07
13e	R^5 = 4-OH	67.46 ± 5.37	9.17 ± 0.52	n.t.[c]
13h	R^5 = 3,5-OH	75.31 ± 4.82	8.72 ± 1.02	n.t.[c]
13i	R^5 = 3,4,5-OH	70.09 ± 2.72	9.32 ± 1.22	n.t.[c]
Resveratrol	—	64.57 ± 3.52	15.10 ± 1.4	5.73 ± 0.27
CQ	—	30.22 ± 2.21	n.t.[c]	0.61 ± 0.05
8-Hydroxyquinoline	—	n.t.[c]	n.t.[c]	2.42 ± 0.21

[a] The thioflavin-T fluorescence method was used. Values are expressed as means ± SD from at least two independent measurements. All the values were obtained with 20 μM of the tested compounds. [b] The thioflavin-T fluorescence method was used. Values are expressed as mean ± SD from at least two independent measurements. [c] n.t. = not tested. [d] The mean ± SD of three independent experiments. Data are expressed in μmol of Trolox equivalent/μmol of tested compound.

respectively). Electron-withdrawing groups were unfavourable for inhibition, as indicated by compounds **13c** and **13d**, which feature a 4-nitro or 4-bromo substitution on the C-ring, showing only a slight Aβ aggregation inhibition at 20 μM.

The complete dose–response curves of compounds with greater than 50% inhibition were also evaluated, and the results are shown in Table 1. The curves show that compounds with *para*-hydroxyl, 3,5-dihydroxyl or 3,4,5-trihydroxyl substitution at the B-/C-ring exhibited similar Aβ aggregation inhibitory activity (IC_{50} value: 8.50 μM–9.32 μM). Among these compounds, compound **10c** most potently inhibited self-mediated $Aβ_{1-42}$ aggregation (**10c**: IC_{50} = 8.50 μM; resveratrol: IC_{50} = 15.10 μM).

Antioxidant activity *in vitro*

The antioxidant activities of the synthesised compounds were determined by measuring the oxygen radical absorbance capacity of fluorescein (ORAC-FL)[34,35] using a vitamin E analogue, Trolox (6-hydroxy-2,5,7,8-tetramethyl chroman-2-carboxylic acid), as a standard. The results in Table 1 indicate that most compounds had potent oxygen radical absorbance capacities, ranging from 1.8- to 3.2-fold of the value of Trolox, except compounds **13c** and **13d**, which feature 4-nitro or 4-bromo substitution on the B-ring, and showed activity of 0.9-fold that of Trolox.

Inhibition of $Aβ_{1-42}$ fibril formation monitored by transmission electron microscopy (TEM)

To further examine the inhibitory ability of the 8-hydroxyquinoline-resveratrol derivatives on $Aβ_{1-42}$ aggregation, we selected **10c**, which showed the most optimal $Aβ_{1-42}$ aggregation inhibition potency (IC_{50} = 8.50 μM) in the TEM assay. Following incubation at 37 °C for 24 h, the sample of $Aβ_{1-42}$ alone aggregated into well-defined Aβ fibrils (Fig. 3b). In contrast, only small bulk aggregates were visible and no characteristic fibrils were observed in the presence of compound **10c** (Fig. 3c) under the same experimental conditions, which proved that **10c** can inhibit $Aβ_{1-42}$ fibrils formation.

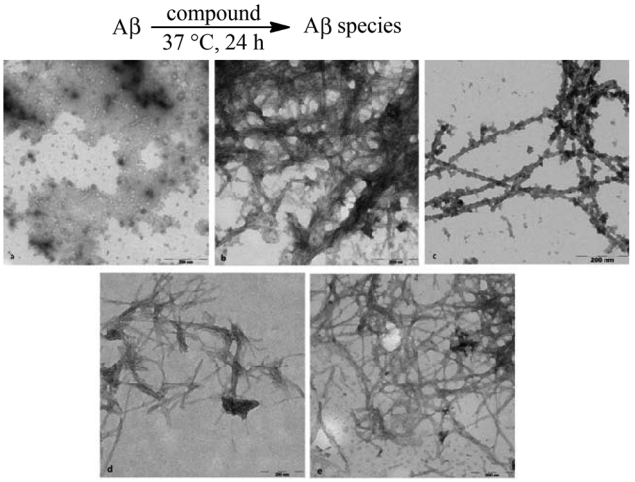

Fig. 3 Top: Scheme of the inhibition experiment. Bottom: TEM images of the samples of $Aβ_{1-42}$ (25 μM) in the presence or absence of compounds (25 μM) (37 °C, 24 h). (a) $Aβ_{1-42}$, 0 h; (b) $Aβ_{1-42}$ alone; (c) $Aβ_{1-42}$ + **10c**; (d) $Aβ_{1-42}$ + resveratrol; (e) $Aβ_{1-42}$ + CQ.

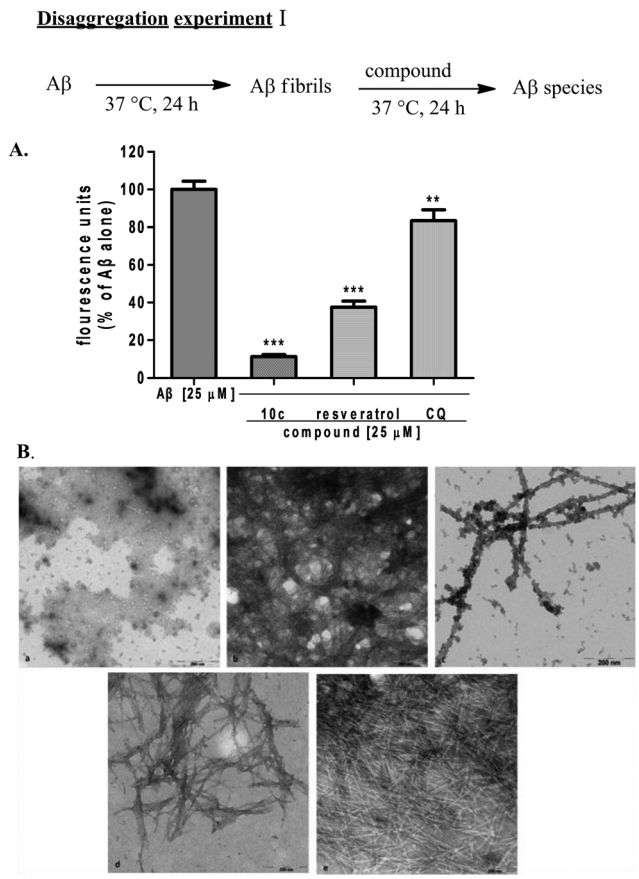

Fig. 4 Top: Scheme of the disaggregation experiment. Bottom: Disaggregation of self-induced $Aβ_{1-42}$ aggregation fibrils by **10c**, resveratrol and CQ ([$Aβ_{1-42}$] = [**10c**] = [resveratrol] = [CQ] = 25 μM, 37 °C, 24 h). (A) Results of the ThT binding assay. Statistical comparisons with control ($Aβ_{1-42}$ alone) were performed by a one-way ANOVA followed by the Dunnett's multiple comparison test using GraphPad Prism 5.0 Software (levels of significance $^{**}p < 0.01$, $^{***}p < 0.001$); (B) TEM images of samples. (a) $Aβ_{1-42}$, 0 h; (b) $Aβ_{1-42}$ alone; (c) $Aβ_{1-42}$ + **10c**; (d) $Aβ_{1-42}$ + resveratrol; (e) $Aβ_{1-42}$ + CQ.

Disaggregation of self-mediated $Aβ_{1-42}$ aggregation fibrils by 10c

The disaggregation ability of **10c** toward the self-mediated Aβ aggregation of fibrils was assayed as follows. First, Aβ fibrils were generated by incubating fresh Aβ (25 μM) for 24 h at 37 °C (Fig. 4b). Compound **10c** (25 μM) was then added to the sample before incubating for another 24 h at the same temperature. The ThT binding assay and examination by TEM (Fig. 4c) showed that **10c** effectively disaggregates Aβ fibrils (88.73% disaggregation at 25 μM as determined by the ThT binding assay).

Metal-chelating properties of compound 10c

The ability of compound **10c** to chelate biometals, such as copper(II), iron(II) and zinc(II), was investigated by UV-vis

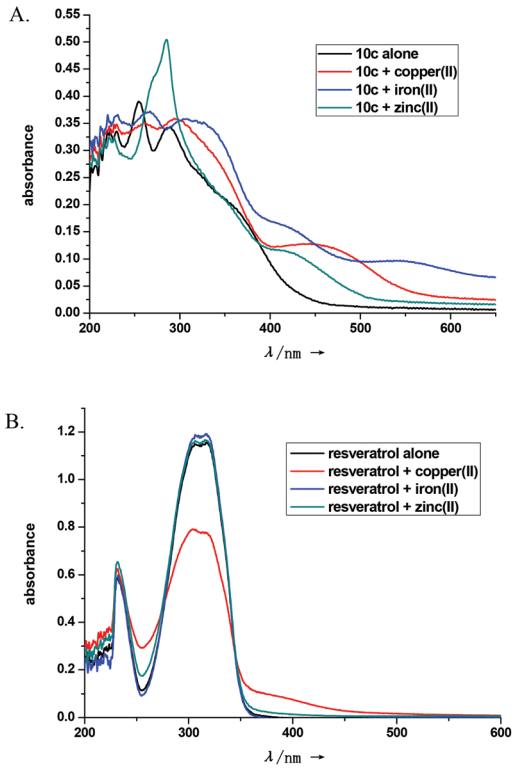

Fig. 5 UV spectra of compound **10c** (A) and resveratrol (B) (40 μM) alone and in the presence of 20 μM $CuSO_4$, $FeSO_4$ or $ZnCl_2$. All the solutions were prepared using a HEPES buffer solution (20 mM HEPES, 150 mM NaCl, pH 7.4).

spectrometry,[36] and the results are shown in Fig. 5A. The specific absorbance peaks of **10c** can be seen at 254 and 290 nm.

After copper(II) was added to the solution of **10c**, specific absorbance at 254 nm shifted to 260 nm, the peak at 290 nm shifted to 294 nm, and a new peak was observed at 445 nm. These changes in absorbance indicate the formation of a **10c**–copper(II) complex. Similarly, the specific absorption of the **10c**–iron(II) complex was shifted to a maxima at 261 nm and 309 nm, and one new absorption peak at 537 nm was observed. When the same experiment was performed using **10c** and zinc(II) to form **10c**–zinc(II), two specific absorptions overlaid at 285 nm without the generation of new peaks. In addition, we evaluated the chelating ability of resveratrol to biometals, such as copper(II), iron(II) and zinc(II), by UV-vis spectrometry. As shown in Fig. 5B, resveratrol interacts strongly with copper(II) but only weakly with iron(II) and shows almost no interaction with zinc(II), which is in agreement with the reported literature.[26]

To determine the stoichiometry of the complex **10c**–copper(II), a series of solutions that maintains the total concentrations of compound **10c** and $CuSO_4$ constant but vary their proportions were prepared according to the Job's method.[37,38] UV spectroscopy was used to determine the absorbance of the $CuSO_4$ complex and **10c** at different concentrations. As indicated in Fig. 6, plotting the absorbance changes at 445 nm yielded two

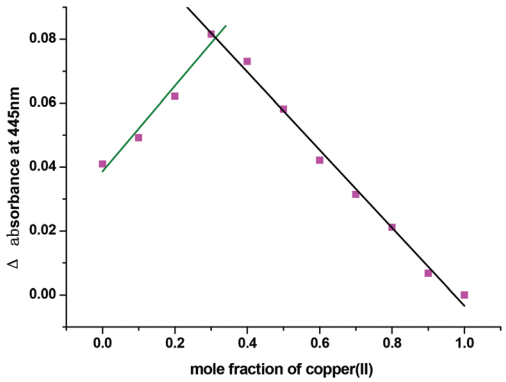

Fig. 6 Determination of the stoichiometry of complex **10c**–copper(II) by the Job's method.

straight lines, intersecting at a mole fraction of 0.32, indicating a 2 : 1 stoichiometry for complex **10c**–copper(II).

The effects of compound 10c on copper(II)-induced $A\beta_{1-42}$ aggregation

To investigate the effects of **10c** on metal-induced Aβ aggregation, we examined the inhibitory activity of compound **10c** on copper(II)-induced $A\beta_{1-42}$ aggregation and the disaggregation effects of **10c** on copper(II)-induced $A\beta_{1-42}$ aggregation fibrils. The ThT binding assay and transmission electron microscopy (TEM) were used to identify the degree of Aβ aggregation.

The results in Fig. 7 indicate that copper(II) accelerates the aggregation of Aβ. The fluorescence of Aβ treated with copper(II) is 1.63 times that of Aβ alone, according to the ThT binding assay. In contrast, the fluorescence of Aβ treated with copper(II) and the test compounds decreased significantly (fluorescence after treatment with **10c**, resveratrol and CQ was 21.93%, 42.82% and 54.13%, respectively), which indicated that these compounds could reduce the rate of Aβ aggregation treated with copper(II). TEM images demonstrated that the Aβ aggregates treated with copper(II) were significantly more intense than the Aβ aggregates alone but the Aβ aggregates obviously decreased when **10c**, resveratrol and CQ were added to the samples, which was consistent with the ThT binding assay results.

Disaggregation of copper(II)-induced $A\beta_{1-42}$ aggregation fibrils by 10c

The disaggregation studies of copper(II)-induced $A\beta_{1-42}$ aggregation fibrils by **10c** are shown in Fig. 8. Compound **10c**, resveratrol and CQ (50 μM) were added individually to Aβ fibrils that were generated by reacting Aβ with 1 equiv. of copper(II) for 24 h at 37 °C under constant agitation. The ThT binding assay indicated that all the compounds could disaggregate Aβ fibrils at 50 μM (percentage of disaggregation was as follows: **10c**, 84.46%; resveratrol, 82.83%; CQ, 43.13%). Fig. 8c shows the visualisation of the Aβ species by TEM, and clearly indicates that **10c** was capable of disassembling the Aβ fibrils resulting from copper(II)-induced aggregation.

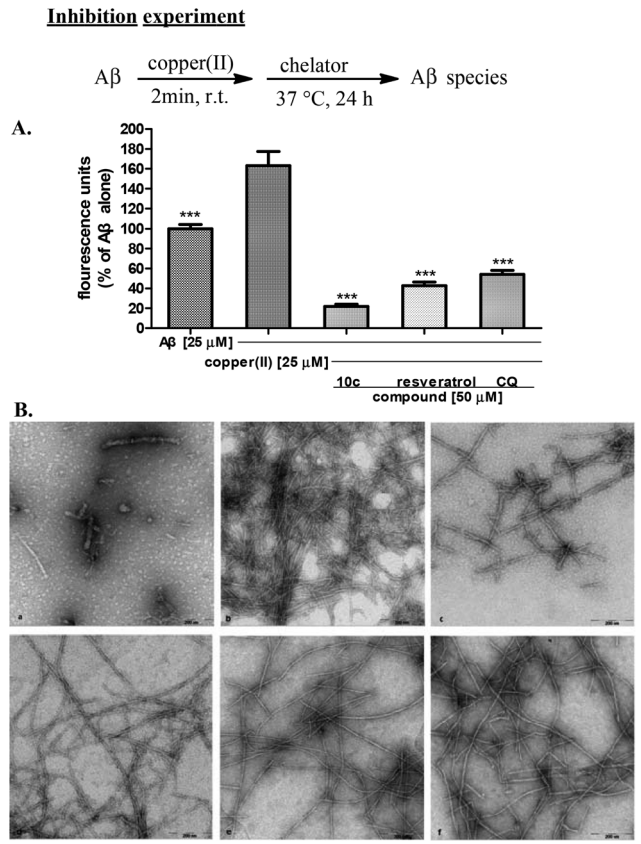

Fig. 7 Top: Scheme of the inhibition experiment. Bottom: Inhibition of copper(II)-induced $A\beta_{1-42}$ aggregation by **10c**, resveratrol and CQ ([$A\beta_{1-42}$] = copper(II) = 25 μM, [**10c**] = [resveratrol] = [CQ] = 50 μM, 37 °C, 24 h). (A) Results of the ThT binding assay. Statistical comparisons with control ($A\beta_{1-42}$ aggregation in the presence of copper(II)) were performed by a one-way ANOVA followed by the Dunnett's multiple comparison test using GraphPad Prism 5.0 Software (level of significance ***$p < 0.001$). (B) TEM images of samples. (a) $A\beta_{1-42}$, 0 h; (b) $A\beta_{1-42}$ + copper(II); (c) $A\beta_{1-42}$ + copper(II) + **10c**; (d) $A\beta_{1-42}$ + copper(II) + resveratrol; (e) $A\beta_{1-42}$ + copper(II) + CQ; (f) $A\beta_{1-42}$ alone.

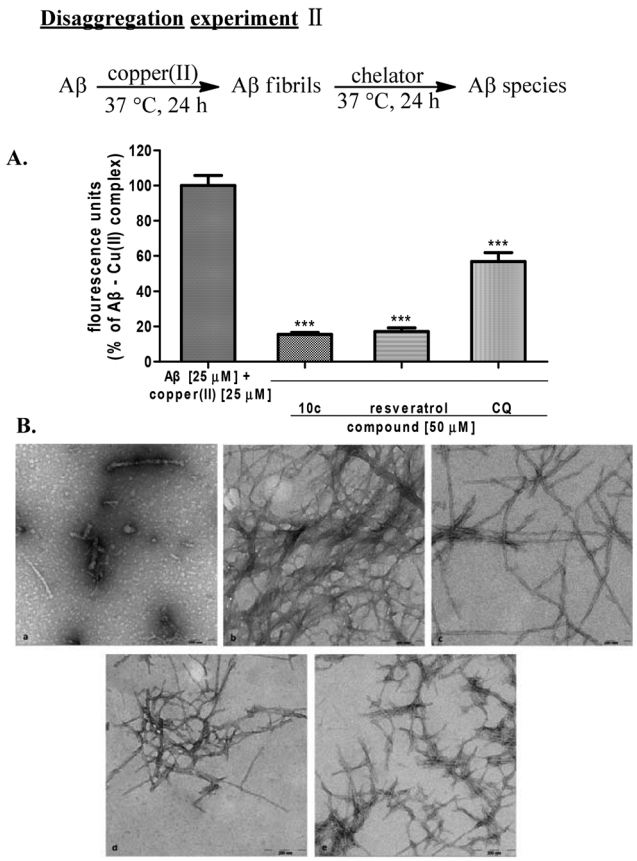

Fig. 8 Top: Scheme of the disaggregation experiment. Bottom: Disaggregation of copper(II)-induced $A\beta_{1-42}$ fibrils by **10c**, resveratrol and CQ ([$A\beta_{1-42}$] = copper(II) = 25 μM, [**10c**] = [resveratrol] = [CQ] = 50 μM, 37 °C, 24 h). (A) Results of the ThT binding assay, Statistical comparisons with control (untreated with compound) were performed by a one-way ANOVA followed by the Dunnett's multiple comparison test using GraphPad Prism 5.0 Software (level of significance, ***$p < 0.001$); (B) TEM images of samples. (a) $A\beta_{1-42}$, 0 h; (b) $A\beta_{1-42}$ + copper(II); (c) $A\beta_{1-42}$ + copper(II) + **10c**; (d) $A\beta_{1-42}$ + copper(II) + resveratrol; (e) $A\beta_{1-42}$ + copper(II) + CQ.

Ability to halt copper redox cycling *via* metal complexation

As reported, redox-active Cu(II) is implicated in the generation of ROS, leading to an increase in oxidative stress, which is a proposed neuropathology of AD. Therefore, we utilised the Cu–ascorbate redox system (Scheme 3), described by Faller and co-workers, as a model to determine whether the ligand **10c** could halt copper based redox activity under aerobic conditions.[39] The production of hydroxyl radicals (OH$^{\bullet}$) by copper redox cycling in the presence of ascorbate was measured by co-incubation with coumarin-3-carboxylic acid (CCA), which generates fluorescent 7-hydroxy-CCA in the presence of OH$^{\bullet}$. As shown in Fig. 9, the OH$^{\bullet}$ in the copper–ascorbate system increases steadily with time and reaches a plateau at approximately 12 min. When **10c** was coincubated with the Cu–ascorbate system, this process was prevented almost entirely, indicating that the ligand is capable of halting copper redox cycling involved in oxidative stress *via* metal complexation.

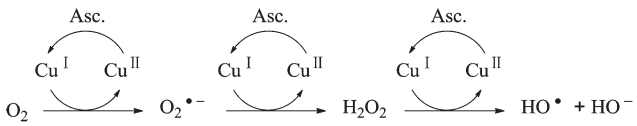

Scheme 3 Production of hydroxyl radical (OH$^{\bullet}$) by copper redox cycling in the presence of ascorbate.

Prediction of the BBB penetration and absorption of compound 10c and 10d

Brain penetration is an essential element for successful anti-AD drugs.[40] To evaluate the 'drug-like-quality' and brain penetration ability of the synthetic compounds, we used Lipinski's rules[41] and calculated log BB using the equation $\log BB = -0.0148 \times PSA + 0.152 \times c\log P + 0.130$ as a criteria. The results in Table 2 indicate that compound **10c** fulfils the necessary drug-like and prediction of brain penetration criteria.

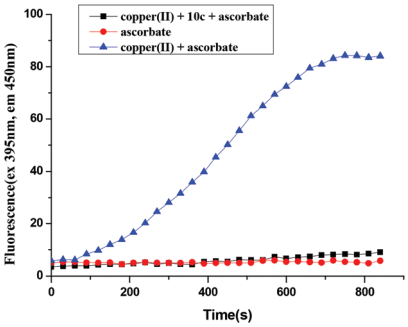

Fig. 9 Fluorescence intensity of the copper–ascorbate and copper–ascorbate–**10c** system. CCA [50 μM] and ascorbate [150 μM] were incubated in each system. [Cu(II)] = [5 μM], [**10c**] = 15 μM. PBS buffer, pH = 7.4.

In vitro blood–brain barrier permeation assay

The parallel artificial membrane permeation assay (PAMPA-BBB) for predicting passive BBB permeation was also performed for our compounds. This method developed by Di *et al.*[43] was capable of identifying compounds as either BBB permeable or non-permeable with high success, high throughput, and reproducibility. First, the *in vitro* permeability (P_e) of 13 quality control standards (with known BBB permeability) were determined *via* a lipid extract of porcine brain using phosphate buffered saline (PBS)–EtOH (70 : 30). The experimental data *versus* bibliographic values showed a good linear correlation, P_e(exp.) = 1.4574P_e(bibl.)–1.0773 (R^2 = 0.9427) (see ESI Fig. S1†). From this equation and by considering the limit established by Di *et al.* for blood–brain barrier permeation, permeability values of over 4.7 × 10^{-6} cm s^{-1} (PBS–EtOH, 70 : 30) were considered sufficient for compounds to cross the BBB (see ESI Table S1†). The selected compounds were then tested in the PAMPA-BBB assay. The results (Table 3) showed that compound **10c** could cross BBB but resveratrol could not. Comparing the permeability values of **10c** and **10d**, it appears that increasing number of hydroxyl groups are against crossing the BBB.

Acute toxicity of compound 10c

To investigate the safety profile of 8-hydroxyquinoline-resveratrol derivatives, the acute toxicity of **10c** was determined in KM mice at doses of 0, 677, 1333, and 2000 mg kg^{-1} (each group, n = 5) by oral administration. No signs of acute toxicity were observed at these doses within the first 4 h after administration, and no animal died in the following 14 days. All the mice were sacrificed on the 14th day of drug administration and were examined macroscopically for any possible damage to the heart, liver, and kidneys. The results showed that the animals treated with compound **10c** did not show any acute toxicity and mortality, either immediately or during the post-treatment period. Furthermore, no significant abnormal changes were observed during the experimental period in terms of water or food consumption or body weight. Therefore, compound **10c** was proven to be non-toxic and well-tolerated at doses of up to 2000 mg kg^{-1}.

Table 2 Physical properties and prediction of BBB penetration and absorption of **10c** and **10d**

Calculation[a]	**10c**	**10d**	Lipinski's rules
MW	263.29	279.29	≤450
C log *P*	3.52	3.28	≤5.0
HBA	3	4	≤10
HBD	2	3	≤5
PSA	52.89	73.71	≤90
Log BB[b]	−0.12	−0.46	≥−1.0
Absorption level[c]	0	0	

[a] MW: molecular weight; *c* log *P*: calculated logarithm of the octanol–water partition coefficient; HBA: hydrogen-bond acceptor atoms; HBD: hydrogen-bond donor atoms; PSA: polar surface area. [b] Compounds with log BB > 0.3 are able to readily cross the BBB, compounds with log BB < −1.0 are only poorly distributed to the brain. [c] Data are predicted by discovery studio 2.1 soft (Accelrys). 0: good absorption, 1: moderate absorption, 2: low absorption, 3: very low absorption.[42]

Table 3 Permeability results (P_e 10^{-6} cm s^{-1}) from the PAMPA-BBB assay for selected 8-hydroxyquinoline-resveratrol derivatives with their predicted penetration into the CNS

Compounds	Permeability (P_e 10^{-6} cm s^{-1})[a]	Prediction
10c	14.7 ± 1.4	CNS+
10d	4.8 ± 0.4	CNS+
Resveratrol	1.05 ± 0.05	CNS−

[a] Values are expressed as mean ± SD of three independent experiments.

Conclusion

Based on the knowledge that resveratrol possesses a variety of bioactivities, we used a fusing strategy to develop a novel series of compounds containing the pharmacophores of resveratrol and clioquinol as multi-target agents for the treatment of AD. Among the synthesised compounds, **10c** exhibited good inhibition of self-induced Aβ aggregation and the ability to disassemble the well-structured Aβ fibrils generated by self-induced Aβ aggregation, both of which can be attributed to the features of resveratrol. In addition, as a result of the 8-hydroxyquinoline moiety, **10c** showed good metal-chelating ability and the ability to inhibit copper(II)-induced Aβ aggregation and disassemble Aβ fibrils generated by copper(II)-induced Aβ aggregation. Furthermore, **10c** exhibited very potent antioxidant activity compared to Trolox. When tested for toxicity in mice, **10c** showed no acute toxicity at doses of up to 2000 mg kg^{-1}. Moreover, according to a parallel artificial membrane permeation assay, **10c** can cross the blood–brain barrier (BBB). In summary, these results show that compound **10c** is worthy of further studies directed toward the development of novel drugs for the treatment of AD.

Acknowledgements

We thank the National Natural Science Foundation of China (no. 21302235, 20972198), Ph.D. Programs Foundation of

Ministry of Education of China (20120171120045), and Distinguished Young Talents in Higher Education of Guangdong (2012LYM_003) for financially supporting this study.

Notes and references

1 N. C. Berchtold and C. W. Cotman, *Neurobiol. Aging*, 1998, **19**, 173–189.
2 J. Hardy, *Neuron*, 2006, **52**, 3–13.
3 J. Lageé and M. Manuelínez, *J. Alzheimer's Dis.*, 2006, **9**, 15–26.
4 http://www.alz.co.uk/research/files/WorldAlzheimerReport. World Alzheimer Report. 2009, Alzheimer's disease international.
5 G. Pepeu and M. G. Giovannini, *Curr. Alzheimer Res.*, 2009, **6**, 86–96.
6 M. Villarroya, A. G. Garcia, J. Marco-Contelles and M. G. Lopez, *Expert Opin. Invest Drugs*, 2007, **16**, 1987–1998.
7 E. Scarpini, P. Scheltens and H. Feldman, *Lancet Neurol.*, 2003, **2**, 539–547.
8 M. B. H. Youdim and J. J. Buccafusco, *Trends Pharmacol. Sci.*, 2005, **26**, 27–35.
9 A. Cavalli, M. L. Bolognesi, A. Minarini, M. Rosini, V. Tumiatti, M. Recanatini and C. Melchiorre, *J. Med. Chem.*, 2008, **51**, 347–372.
10 J. Hardy and D. J. Selkoe, *Science*, 2002, **297**, 353–356.
11 P. A. Novick, D. H. Lopes, K. M. Branson, A. Esteras-Chopo, I. A. Graef, G. Bitan and V. S. Pande, *J. Med. Chem.*, 2012, **55**, 3002–3010.
12 R. Di Santo, R. Costi, G. Cuzzucoli Crucitti, L. Pescatori, F. Rosi, L. Scipione, D. Celona, M. Vertechy, O. Ghirardi, P. Piovesan, M. Marzi, S. Caccia, G. Guiso, F. Giorgi and P. Minetti, *J. Med. Chem.*, 2012, **55**, 8538–8548.
13 M. Catto, R. Aliano, A. Carotti, S. Cellamare, F. Palluotto, R. Purgatorio, A. De Stradis and F. Campagna, *Eur. J. Med. Chem.*, 2010, **45**, 1359–1366.
14 A. Kumar, L. Moody, J. F. Olaivar, N. A. Lewis, R. L. Khade, A. A. Holder, Y. Zhang and V. Rangachari, *ACS Chem. Neurosci.*, 2010, **1**, 691–701.
15 J. Dong, C. S. Atwood, V. E. Anderson, S. L. Siedlak, M. A. Smith, G. Perry and P. R. Carey, *Biochemistry*, 2003, **42**, 2768–2773.
16 T. A. Bayer, S. Schafer, A. Simons, A. Kemmling, T. Kamer, R. Tepest, A. Eckert, K. Schussel, O. Eikenberg, C. Sturchler-Pierrat, D. Abramowski, M. Staufenbiel and G. Multhaup, *Proc. Natl. Acad. Sci. U. S. A.*, 2003, **100**, 14187–14192.
17 A. I. Bush, *J. Alzheimer's Dis.*, 2008, **15**, 223–240.
18 T. Amit, Y. Avramovich-Tirosh, M. B. H. Youdim and S. Mandel, *FASEB J.*, 2007, **22**, 1296–1305.
19 D. J. Bonda, X. Wang, G. Perry, A. Nunomura, M. Tabaton, X. Zhu and M. A. Smith, *Neuropharmacology*, 2010, **59**, 290–294.
20 T. M. Bray, *Proc. Soc. Exp. Biol. Med.*, 1999, **222**, 195.
21 K. Beking and A. Vieira, *Public Health Nutr.*, 2010, **13**, 1403–1409.
22 H. P. Lee, G. Casadesus, X. Zhu, H. G. Lee, G. Perry, M. A. Smith, K. Gustaw-Rothenberg and A. Lerner, *Expert Rev. Neurother.*, 2009, **9**, 1615–1621.
23 H. Y. Zhang, D. P. Yang and G. Y. Tang, *Drug Discovery Today*, 2006, **11**, 749–754.
24 D. J. Boocock, G. E. Faust, K. R. Patel, A. M. Schinas, V. A. Brown, M. P. Ducharme, T. D. Booth, J. A. Crowell, M. Perloff, A. J. Gescher, W. P. Steward and D. E. Brenner, *Cancer Epidemiol. Biomarkers Prev.*, 2007, **16**, 1246–1252.
25 A. R. Ladiwala, J. C. Lin, S. S. Bale, A. M. Marcelino-Cruz, M. Bhattacharya, J. S. Dordick and P. M. Tessier, *J. Biol. Chem.*, 2010, **285**, 24228–24237.
26 A. Granzotto and P. Zatta, *PLoS One*, 2011, **6**, e21565.
27 I. M. Kapetanovic, M. Muzzio, Z. Huang, T. N. Thompson and D. L. McCormick, *Cancer Chemother. Pharmacol.*, 2011, **68**, 593–601.
28 J. Geng, M. Li, L. Wu, J. Ren and X. Qu, *J. Med. Chem.*, 2012, **55**, 9146–9155.
29 M. G. Savelieff, Y. Liu, R. R. Senthamarai, K. J. Korshavn, H. J. Lee, A. Ramamoorthy and M. H. Lim, *Chem. Commun.*, 2014, **50**, 5301–5303.
30 A. Kochi, T. J. Eckroat, K. D. Green, A. S. Mayhoub, M. H. Lim and S. Garneau-Tsodikova, *Chem. Sci.*, 2013, **4**, 4137–4145.
31 S. Lee, X. Zheng, J. Krishnamoorthy, M. G. Savelieff, H. M. Park, J. R. Brender, J. H. Kim, J. S. Derrick, A. Kochi, H. J. Lee, C. Kim, A. Ramamoorthy, M. T. Bowers and M. H. Lim, *J. Am. Chem. Soc.*, 2014, **136**, 299–310.
32 K. M. Lincoln, P. Gonzalez, T. E. Richardson, D. A. Julovich, R. Saunders, J. W. Simpkins and K. N. Green, *Chem. Commun.*, 2013, **49**, 2712–2714.
33 M. Rosini, E. Simoni, M. Bartolini, A. Cavalli, L. Ceccarini, N. Pascu, D. W. McClymont, A. Tarozzi, M. L. Bolognesi, A. Minarini, V. Tumiatti, V. Andrisano, I. R. Mellor and C. Melchiorre, *J. Med. Chem.*, 2008, **51**, 4381–4384.
34 B. Ou, M. Hampsch-Woodill and R. L. Prior, *J. Agric. Food Chem.*, 2001, **49**, 4619–4626.
35 A. Dávalos, C. Gómez-Cordovés and B. Bartolomé, *J. Agric. Food Chem.*, 2003, **52**, 48–54.
36 J.-S. Choi, J. J. Braymer, R. P. R. Nanga, A. Ramamoorthy and M. H. Lim, *Proc. Natl. Acad. Sci. U. S. A.*, 2010, **107**, 21990–21995.
37 S. S. Hindo, A. M. Mancino, J. J. Braymer, Y. Liu, S. Vivekanandan, A. Ramamoorthy and M. H. Lim, *J. Am. Chem. Soc.*, 2009, **131**, 16663–16665.
38 M. a. I. Fernández-Bachiller, C. n. Pérez, G. C. González-Muñoz, S. Conde, M. G. López, M. Villarroya, A. G. García and M. a. I. Rodríguez-Franco, *J. Med. Chem.*, 2010, **53**, 4927–4937.
39 L. Guilloreau, S. Combalbert, A. Sournia-Saquet, H. Mazarguil and P. Faller, *ChemBioChem*, 2007, **8**, 1317–1325.

40 H. van de Waterbeemd and E. Gifford, *Nat. Rev. Drug Discovery*, 2003, **2**, 192–204.
41 D. E. Clark and S. D. Pickett, *Drug Discovery Today*, 2000, **5**, 49–58.
42 W. J. Egan, K. M. Merz and J. J. Baldwin, *J. Med. Chem.*, 2000, **43**, 3867–3877.
43 L. Di, E. H. Kerns, K. Fan, O. J. McConnell and G. T. Carter, *Eur. J. Med. Chem.*, 2003, **38**, 223–232.